Back to Session Subjects

INTERCONNECTING SHAFT FOR THE EUROPEAN TILT ROTOR AIRCRAFT

Andreas Podratzky[1], Heinrich Schweitzer[2]

[1] Eurocopter Deutschland GmbH
81663 München
e-mail: andreas.podratzky@eurocopter.com

[2] Eurocopter Deutschland GmbH
81663 München
e-mail: heinrich.schweitzer@eurocopter.com

ECD-0155-06-PUB

Key words: interconnecting shaft, supercritical shaft, tilt rotor, TRISYD

Abstract: ERICA[1] is a concept of an advanced tilt rotor aircraft. It is presently under development within a multinational consortium funded by the European commission within the 5th framework. One of the critical technology projects is TRISYD[2].

A task of Eurocopter within TRISYD was to develop the interconnecting shaft between the two rotors of ERICA, which provides the necessary torque for the opposite rotor in case of an engine failure. The shaft environment is a torque tube connecting both nacelles. After studying various concepts, a full composite supercritical shaft composed of seven segments was chosen.

As a subtask of TRISYD, a full composite, dynamically downscaled model of the interconnecting shaft was manufactured and tested.

The main characteristics of the downscaling procedure were:

- The full size and the downscaled shaft have similar dynamic characteristics (Cauchy-number).
- The first critical speed in terms of percentage of nominal speed is similar.
- The shafts are manufactured with composite materials.
- The attachments of the downscaled shaft are usual helicopter tail rotor drive shaft components.

Special attention was paid to the damping behaviour of the test bench arrangement. On the test bench, the damping is achieved by elastomeric bearing suspensions with anisotropic stiffness behaviour in different radial shaft directions. The result is a very smooth behaviour of the shaft with reduced deflections after passing the first critical speed. Defined shaft unbalance, angular deflections and bench damping variations were tested afterwards.

These investigation results shall be used for the detailed design of ERICA's interconnecting shaft and might be used for other supercritical shaft applications.

[1] ERICA = Enhanced Rotorcraft Innovative Concept Achievement
[2] TRISYD = Tilt Rotor Interconnecting Drive SYstem Development

INTRODUCTION

The TRISYD project [1] is one of six critical technology projects funded by the European Commission within the 5th Framework Program. The aim of the program is to develop technologies for an advanced tilt rotorcraft. The project structure is depicted in figure 1.

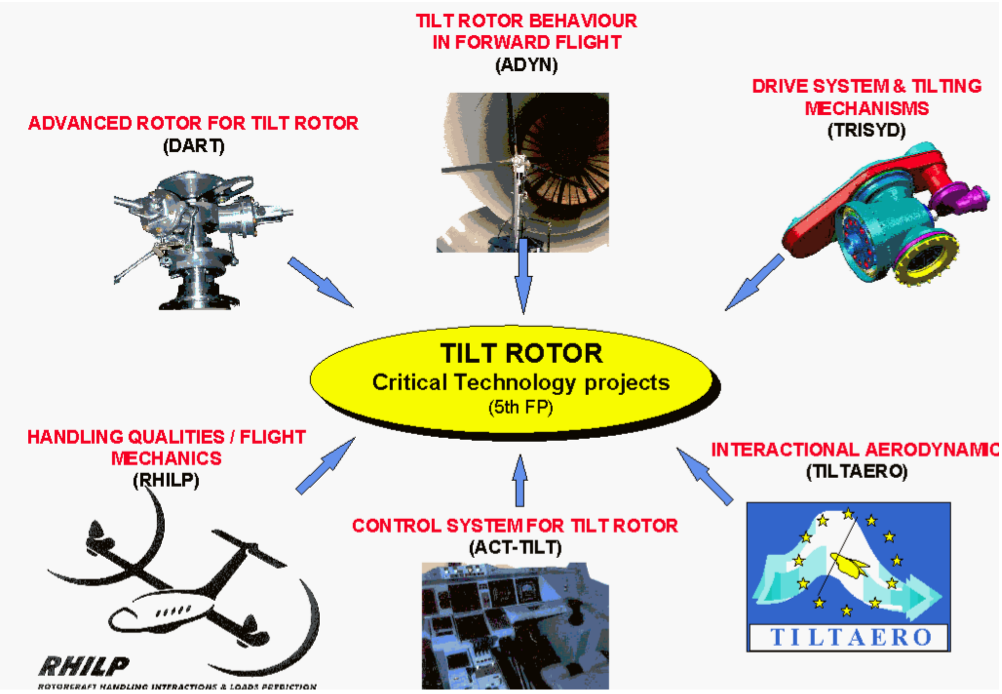

Figure 1: Critical projects within the 5th Tilt Rotor Framework Program

TRISYD is managed by a consortium of aeronautical industry companies in collaboration with universities and research centers. The program is oriented towards the study and the definition of the drive system for an advanced European tilt rotor configuration called ERICA (Enhanced Rotorcraft Innovative Concept Achievement; see figure 2 and [1]).

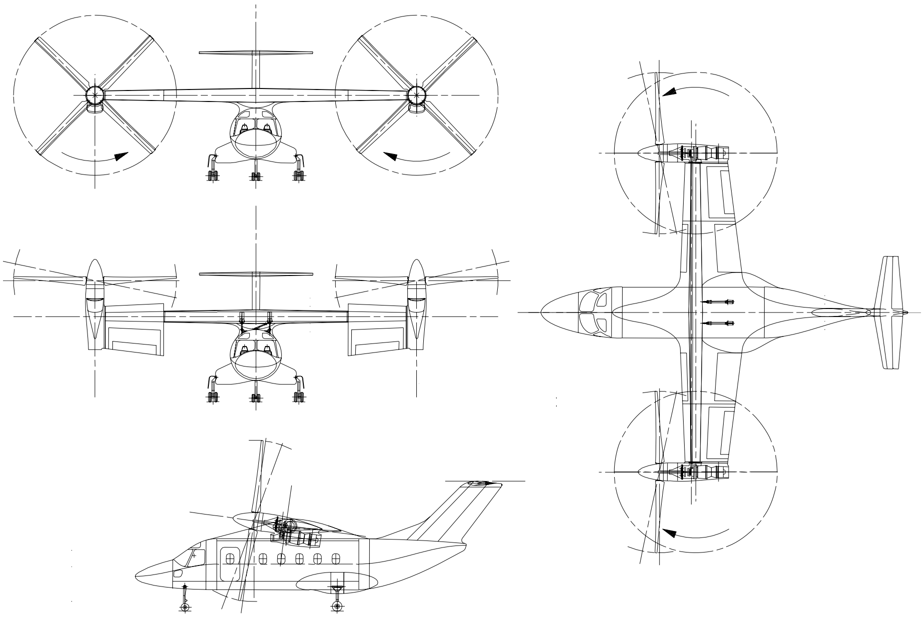

Figure 2: Sketch of the ERICA tilt rotor aircraft with nacelles connecting torque tube

ERICA defines an innovative second generation tilt rotor architecture, which has the following characteristics:

- A small rotor diameter, which offers a reasonable hover performance as well as the possibility to take-off and land in aircraft mode.
- An outboard portion of the wing, located in the downstream of the rotors, with the ability to tilt independently of the nacelles (figure 3)
- A full span single tubular spar ("torque tube") provides all the wing structural integrity of the tilting outboard portions and synchronizes the tilting of the two nacelles (figure 2, right view and figure 4).

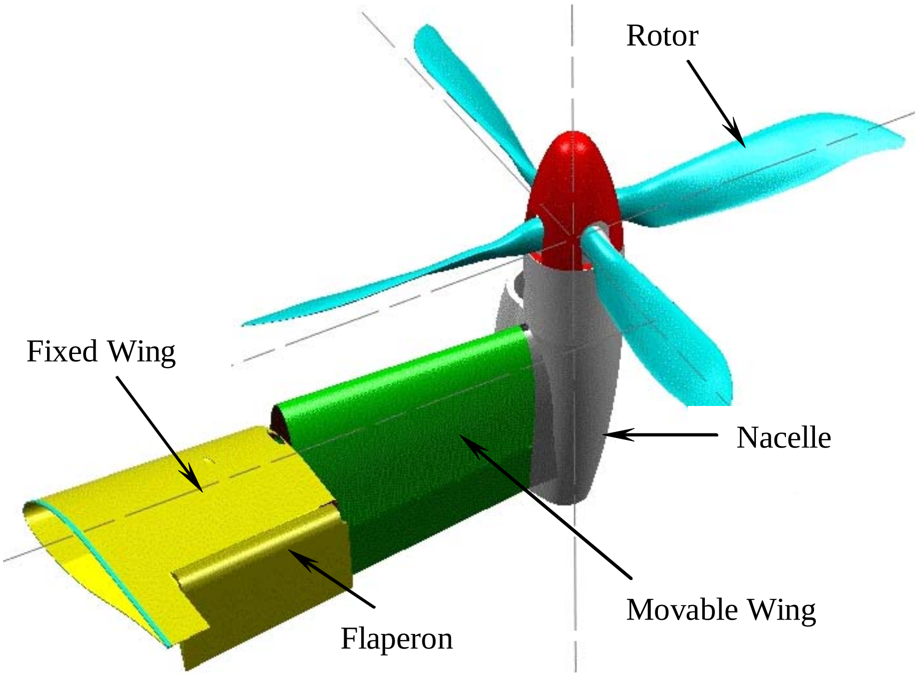

Figure 3: ERICA wing concept with nacelle

The torque tube rigidly connects the two nacelles. It sustains the interconnecting shaft and transmits bending loads from the connection fixed wing to the movable wing. It also transmits the bending and torsional loads from the nacelle to the airframe (figure 4).

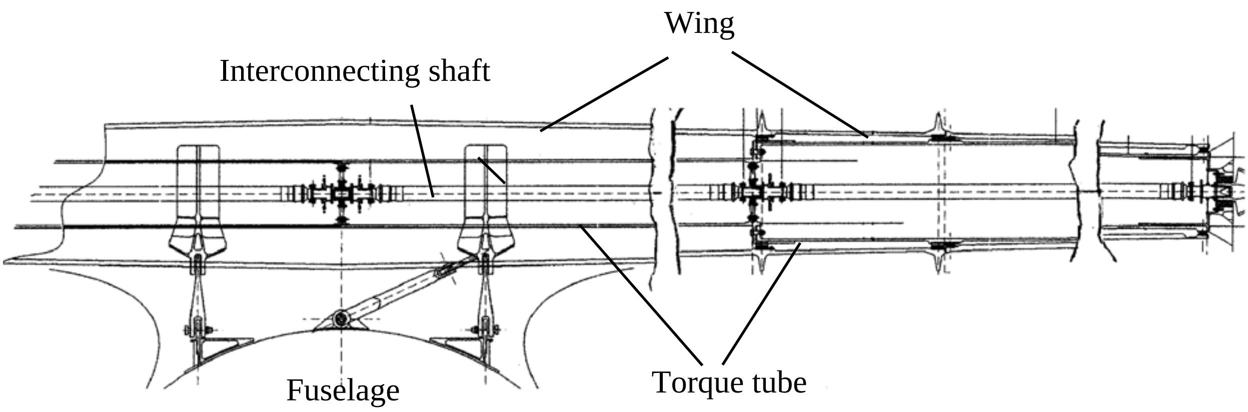

Figure 4: Environment of the interconnecting shaft including torque tube and mid-wing fuselage area

The main purpose of the torque tube is to synchronise the nacelles by establishing a rigid connection. The tilting of the nacelles is performed by simply rotating the torque tube.

1 THE INTERCONNECTING SHAFT

1.1 General Purpose and Definition

The interconnecting shaft (ICS[3]) of the ERICA tilt rotor aircraft connects the two gearboxes. Figure 5 shows the proprotor gearbox with the interconnecting shaft for the left wing side.

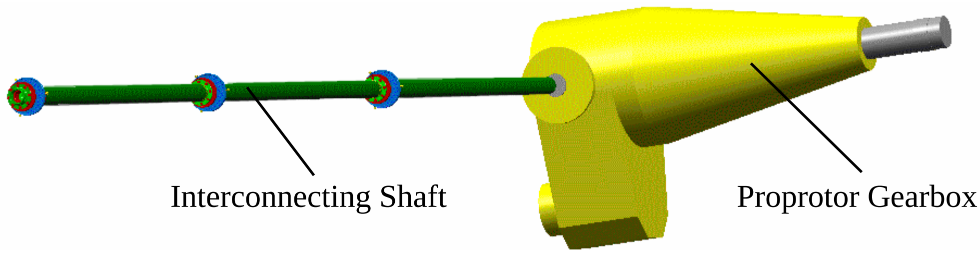

Figure 5: Interconnecting shaft with a nacelle (schematic) for the left wing side

Its main purpose is to provide the necessary driving torque for the opposite rotor in case of an engine failure. The shaft also synchronises the rotor speeds of the two rotors, thus minimizing unintended yaw motions due to differential torque in helicopter mode.

1.2 Airworthiness Requirements

One of the tasks within the TRISYD project was to identify the necessary requirements for the ICS. The ICS shall comply with the JAR/FAR rules, part 25 and/or part 29, as applicable. The airworthiness requirements are identified in table 1.

Table 1: Applicable airworthiness requirements

REQUIREMENT [7], [8]	**DESCRIPTION**
	Design and Construction - General
§ 601	Design
§ 623	Bearing Factors
§ 625	Fitting Factors
	Power Plant - Rotor Drive System
§ 917	Design
§ 923	Rotor Drive System and Control Mechanism Tests
§ 927	Additional Tests
§ 931	Shafting Control Speeds
§ 935	Shafting Joints
	Equipment - General
§ 1309	Equipment, Systems & Installations

These requirements where considered during the design process of the shaft.

[3] ICS = Interconnecting Shaft

1.3 Analysis of Existing Long Drive Shafts

In a first step, long drive shaft applications in rotor aircrafts were investigated. Special attention was paid to tilt rotor applications and to modern helicopter tail rotor drive shafts. The main solutions are presented in table 2.

Table 2: Basic parameters of long drive shafts

	Tilt rotor aircrafts		Helicopters	
Parameter	**BA609 [4]**	**V22 [10]**	**Tiger TRS**[4]	**NH90 TRS**
Shaft design	subcritical	subcritical	supercritical	supercritical
Shaft material	CFRP[5]	composite	aluminium	steel
Shaft outer diameter - mm	~76	~160	~84	~95
Overall shaft length - m	10.36	13.97	~6.50	7.9
Length of shaft segments - m	8x1.20	6x1.45	2 x 3.25	2.20 + 2.18
	+2x0.38	+1.09+2x1.22		2.27 + 0.89
Number of couplings	14	10	4	7
Max. transmitted power - kW	1127	5034	~600	~700
Shaft speeds				
- Nominal speed (100%) - rpm	8300	6574	5050	5300
- Maximum transient speed - %	110%	110%	123%	117%
- In Airplane Mode - %	84%	84%	85%	75%

Supercritical shafts are passing one or more natural bending frequencies of the system. They are usually made of long shaft segments with a low number of bearing supports. Therefore they can be designed more lightweight. Special care must be paid to the applicable speed range. The shaft natural frequencies must be outside of this speed range.

Supercritical shaft applications are not common on tilt rotor aircrafts while they are more and more used on helicopter tail rotor drive shaft applications.

1.4 Basic Dynamic Parameters and Relationships

The basic dynamic relations presented in this chapter are based on reference [6]. The purpose of the shaft dynamic calculations is to determine the influence of the following parameters:

- Diameter and wall thickness
- Number of shaft segments
- Length of shaft segments
- Material (elastic and inertial properties)
- Nominal rotational frequency

The basic formula for this analysis is the "*i*-th" natural bending frequency f_i of a uniform beam:

$$f_i = \frac{\lambda_i^2}{2\pi L^2}\sqrt{\frac{EI}{m'}} \qquad (1)$$

where *i* is the index of the natural bending mode, *L* is the length of the shaft, m' is its

[4] TRS = Tail Rotor Shaft

[5] CFRP = Carbon Fibre Reinforced Plastic

distributed mass per meter and EI is the bending stiffness of the shaft cross section. The parameter λ_i characterizes the influence of the constraints at the shaft ends. E.g. for a beam supported by stiff bearings at both ends (pivot joint), it has the value

$$\lambda_i = \pi\, i \tag{2}$$

The distributed mass of a hollow shaft is

$$m' = \pi \rho (r_a^2 - r_i^2)\,. \tag{3}$$

The bending stiffness of a hollow shaft is

$$EI = \frac{E\pi}{4}(r_a^4 - r_i^4) = \frac{E\pi}{4}(r_a^2 - r_i^2)(r_a^2 + r_i^2)\,. \tag{4}$$

where r_a and r_i are the outer and inner radius.
Combining the equations equation (3) and (4) leads to:

$$\frac{EI}{m'} = \frac{E}{4\rho}(r_a^2 + r_i^2) \approx \frac{E}{2\rho} r_m^2 \tag{5}$$

with the mean shaft radius

$$r_m = \frac{r_a + r_i}{2}\,.$$

The formula takes the following form:

$$f_i = \frac{\lambda_i^2}{2\pi L^2} r_m \sqrt{\frac{E}{2\rho}} \tag{6}$$

In this formula the following basics of critical shaft speeds with respect to bending are visible:

- The constraints at the shaft ends and the beam length appear squared in the formula; they are the strongest parameters.
- The frequencies depend linearly from the mean shaft diameter, whereas in the first approximation, there is no influence of the wall thickness.
- Typical is the linear dependency from the parameter $\sqrt{E/\rho}$.

1.5 Environment of the ERICA Interconnecting Shaft

The environment of the ICS is determined by the ERICA concept (figure 4).

The following aspects had to be considered for the shaft definition:

- The geometry of the ERICA tilt rotor aircraft and its two rotors
- The operational environment of the ICS (dimensions of the fixed and movable parts of the wing, and of the torque tube)
- The necessary power (max. OEI[6] case with 1380 kW) and speed range of the two rotors / engines (both in helicopter and in aircraft mode)
- Total length of the shaft of approximately 14 m
- A reduced specific shaft weight

[6] OEI = One Engine Inoperative

During the development of the ICS, additional parameters and conditions had to be considered and analysed:

- The shaft design: subcritical or supercritical shaft[7] design
- The nominal frequency the ICS at 100% in helicopter mode (initially predefined: 150 Hz)
- Material of the shaft, i.e. metallic or CFRP shaft
- The ICS layout, e.g. numbers of bearings and couplings, shaft diameter and wall thickness

So the first task was to figure out a "reasonable" basic design of this shaft. In the following a short outline of this pre-design process will be given.

1.6 Design Considerations

The main design requirement for the TRISYD interconnecting shaft is that its operational frequency must be separated adequately from any critical bending frequency over the whole frequency range. This means:

- For subcritical shafts the first critical bending frequency must be well above its maximum design frequency
- For supercritical shafts the whole used frequency range must fit into a "bending frequency gap" between two consecutive bending frequencies.

The frequency range specified by ERICA was as follows.

Table 3: Frequency range of ERICA rotor and drive system

Mode	Shaft Rpm
Power-on helicopter mode:	104 % Ω_n [8]
Power-off (steady):	106 % Ω_n
Power-off (Autorotation / transient):	121 % Ω_n
Power-on aircraft mode:	77 % Ω_n
Minimum transient in aircraft mode:	68.5 % Ω_n

Thus a large rpm range of the tilt rotor must be considered when designing a supercritical interconnecting shaft, because a supercritical shaft should only be operated in the frequency gap between two adjacent natural frequencies defined by minimum speed in aircraft mode and maximum speed in helicopter mode for autorotation. Any passing of or operation near a critical speed (e.g. during conversion from H/C[9] mode to A/C[10] mode and vice versa) must be avoided. This explains why the presently flying tilt rotor aircrafts have subcritical shafts while modern helicopter tail rotor shafts are often supercritical (table 2).

The "adequate" rpm margin according to JAR Part 29 rules for this case (see [9]) is 20% for subcritical shafts when using a detailed analytical model of the shaft for compliance purpose. For supercritical shafts, the JAR rules do not prescribe a margin; they only demand an adequate damping device for crossing the critical speed(s) (see [2]).

[7] A shaft is called "supercritical", if its operational rotational speed is higher than its first critical bending speed; the critical shaft speeds are the natural shaft bending frequencies.

[8] Ω_n is the nominal speed in helicopter mode (100%).

[9] H/C = Helicopter

[10] A/C = Aircraft

For the analysis a margin of 10% to the two adjacent natural bending frequencies of the shaft was chosen and considered adequate. Thus, the shaft design had to meet the following criteria:

- For a subcritical shaft the first natural bending frequency had to be at least 20% over the maximum shaft speed, i.e. $\omega_1 \geq 145\,\%\ \Omega_n$
- For a supercritical shaft, a “natural frequency gap” from 10% under the minimum and 10% over the maximum shaft speed had to exist, i.e. $\omega_{lower} < 62\%\ \Omega_n$ and $\omega_{upper} > 133\%\ \Omega_n$.

The preliminary calculations yielded the natural bending frequencies of some basic shaft versions. The calculations were performed with Eurocopter’s FORTRAN program “SHAFT”, a classic transfer matrix program based on [11]. The following assumptions and parameter variations were used:

- A shaft with constant cross sectional mass and stiffness properties
- Equally spaced bearings
- Bearings modelled as simple, stiff linear springs without damping
- Flexible couplings with moderate bending stiffness on both sides of the bearings
- Shaft divided into 4, 6 or 8 equally long shaft sections
- Consideration of subcritical and supercritical shaft designs
- Consideration of metallic (aluminium, steel) and CFRP shaft versions
- Nominal shaft frequency varied between 100 and 150 Hz
- Maximum transmitted power for the OEI case: 1380 kW resulting in a maximum torque of 2196 / 1464 Nm for a shaft nominal frequency of 100 / 150 Hz

$$P = M\omega = M\,2\pi\,f \tag{7}$$

The calculations for supercritical shaft variants showed that the shaft bending natural frequencies were not uniformly distributed over the frequency range. They occurred in clusters with distinct gaps between two adjacent frequency clusters having as many frequencies as shaft segments. For a six-segmented shaft this is shown schematically in the following figure.

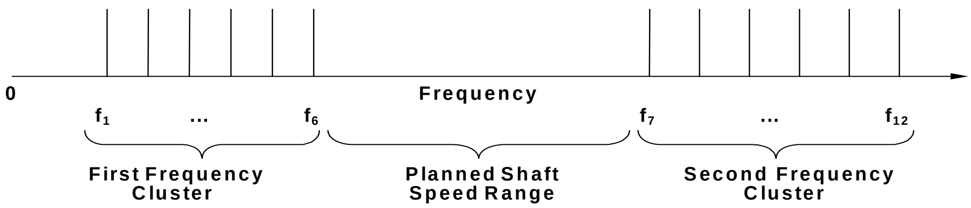

Figure 6: Scheme of bending frequencies of supercritical shaft (with 6 segments)

All frequencies of one cluster are very close together. This gives room for the ERICA frequency range (above and table 3).

The performed calculations showed that the first natural frequency of each of these frequency clusters is almost exactly the same as that of one isolated shaft segment between two bearings according to formula (6).

The stiffness of the shaft bearings also has an influence on the natural frequencies. If it is high enough (i.e. approximately $k > 1\text{x}10^8$ N/m), the results are comparable to that of “perfectly stiff” bearings. With the bearings getting less stiff, the shaft’s natural bending frequencies also start to get lower and lower.

As the ERICA nominal design speed of the interconnecting shaft (initially: 9000 rpm / 150 Hz) seemed pretty high, this analysis also considered the noticeably lower speed of 6000 rpm / 100 Hz, in order to get two extremes for the resulting shaft properties.

In all cases the CFRP shaft has a clear advantage over the aluminum shaft, which can mainly be attributed to its combination of a noticeably lower material density with comparable stiffness properties.

The main investigation results are presented in table 4. With these preliminary results, the preliminary design phase of the TRISYD ICS was completed.

Table 4: Overall weights and diameters of ICS designs (weight without bearings / couplings)

Shaft Design	**Overall Weight / Diameter**			
	Aluminium Shaft		**CFRP Shaft**	
	100 Hz	150 Hz	100 Hz	150 Hz
Subcritical Design (8 Segments)	62.8kg / 170mm	96.6kg / 260mm	21.4kg / 130mm	33.3kg / 200mm
Supercritical Design (6 Segments)	24.4kg / 68mm	38.7kg / 106mm	**16.2kg / 80mm**	16.5kg / 84mm
Supercritical Design (4 Segments)	56.8kg / 154mm	89.1kg / 240mm	16.9kg / 100mm	29.9kg / 180mm

Due to the weight advantage, the supercritical 6-segmented CFRP solution was chosen.

1.7 Detailed Shaft Design

Within the detailed design phase, the final layout of the shaft was defined. The dynamic shaft model was detailed and many design iterations were performed to fit the shaft dynamic behavior to the frequency gap. The following shaft parameters were analyzed:

- Shaft outer diameter and wall thickness
- Shaft CFRP composition: percentage of 0° and ±45° prepreg layers (see [5])

As an example, figure 7 shows the influence of the shaft outer diameter for a shaft with 41% of ±45° prepreg layers. The shaft wall thickness remained unchanged. The required frequency range is denoted with f_{min} and f_{max}.

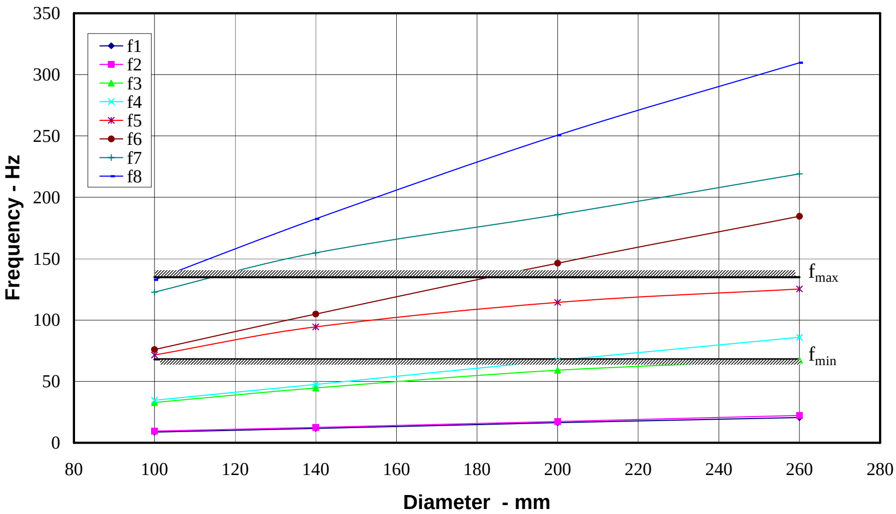

Figure 7: Influence of the shaft outer diameter on the natural bending frequencies for a shaft with 41% of ±45° prepreg layers and unchanged shaft wall thickness

Over the shown diameter range, there is no available gap free of shaft bending frequencies. Therefore the percentage of ±45° prepreg layers had to be increased up to 60%.

Using the multi-body simulation program SIMPACK (see [3]), a detailed calculation model of the shaft was generated, which was able to simulate run-ups and run-downs, and to analyze the stability behaviour of the shaft.

As a result of the iterative calculations, it was detected that the symmetric and the anti-metric modes of the shaft were different for the six-segment solution. Therefore, a short mid-wing shaft was integrated to dynamically separate the left and right wing span shafts. By this design mean the anti-metric and the symmetric modes of the shaft obtained the same natural frequency. Figure 8 shows one wing segment shaft with the gearbox output pinion and an enlarged view of the mid-wing shaft area.

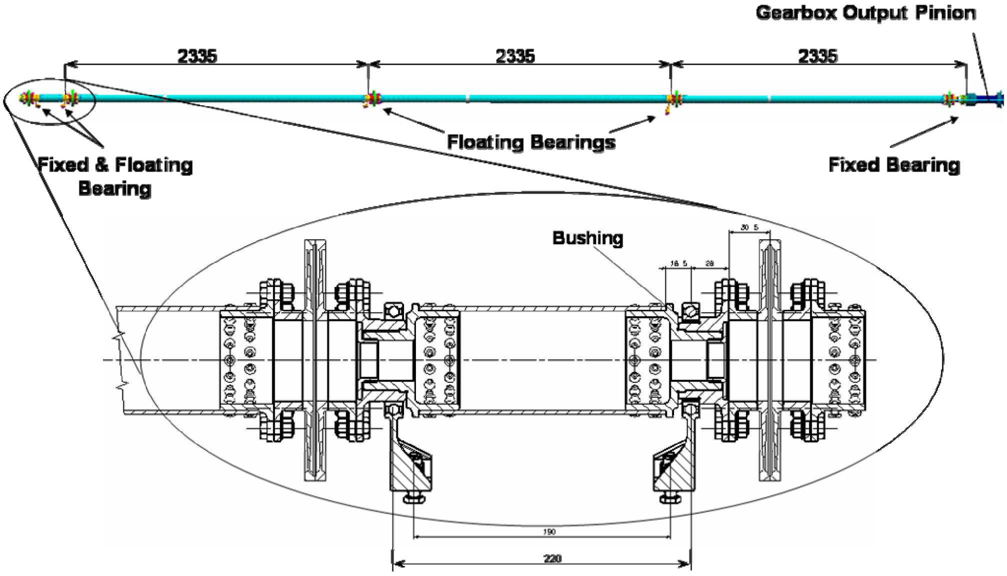

Figure 8: Interconnecting shaft with detailed mid-wing segment

For safety reasons all shaft segments were equipped with a damping device in the middle. The purpose of this device is to limit the radial shaft deflections when passing the critical speeds. In touch with the shafts it damps the shaft vibrations by defined friction forces on the hinged damper arm. Under normal operation conditions, there is no contact between the shaft and the damping device. The damping device is shown in figure 9.

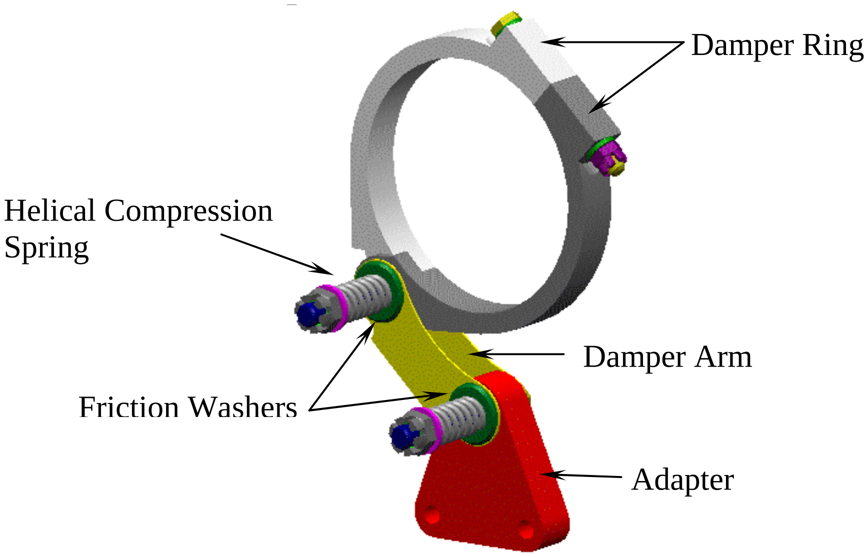

Figure 9: Damping device of the interconnecting shaft

2 DOWNSCALING OF THE INTERCONNECTING SHAFT

2.1 Purpose of Downscaling

One of the main aims of the project “Interconnecting shaft of a tilt rotor aircraft” was to go beyond a “simple” design study for such a shaft by building a test shaft in order to demonstrate the shaft properties. It was decided to manufacture and test a downscaled shaft with dynamically similar properties.

The aim of the downscaling was to perform tests with the shaft while considering a limited budget which would not allow testing the full scale shaft model. The result of this downscaling procedure may lead to a general rule how to combine low cost testing with analytical calculations.

2.2 Preliminary Considerations

For the downscaling procedure several aspects had to be taken into account:

- Simplicity of design
- Use of only one segment instead of seven (six long and one short segment)
- Use of available hardware such as bearings, couplings, manufacturing machines etc.
- ECD knowledge for manufacturing CFRP shafts made from prepreg fabric.

The most important issue was the desired dynamic similarity between the full scale shaft and the model shaft.

The standard parameter describing dynamic similarity is the Cauchy number, which is a measure of the proportion between the elastic (bending) forces, and the inertial forces.
For a rotating shaft it is defined as follows:

$$C = \frac{\Omega^2 \, m' L^4}{E\, I}, \tag{8}$$

where Ω is the rotational speed of the shaft, m' is its distributed shaft mass per meter, L is the free length of the shaft between two suspension points or between two couplings, and EI is the bending stiffness of the shaft cross section.

For two dynamically similar shafts, the parameter C has to have approximately the same value. For the whole length L constant shaft sectional properties were assumed. The full scale shaft with given variations of the cross sectional properties along the shaft length had to be calculated by using averaged properties. The characteristic length L of the full scale shaft used for the calculation of C was the length between two couplings ($L \approx 2.33$ m) of one shaft segment.

The bearings and the flexible couplings were adopted from the tail rotor drive shafts of Eurocopter’s EC135[11] helicopter. This made it advisable to reduce the nominal rotational frequency of the model shaft from 100 to 83 Hz, as required for these components.

Another item adopted from the EC135 manufacturing infrastructure was the inner diameter of the model shaft. By deciding to use the winding machine used for the two short sections of the tail rotor drive shaft system, this parameter was fixed.

Finally, the wall thickness was determined to be approximately 3 mm; a typical value for CFRP shafts, which has proven to be both feasible and reasonable.

---

[11] EC135 = Eurocopter twin engine light helicopter with MTOW = 2910kg

Thus, for the downscaled shaft the following design parameters could be selected within reasonable limits:

- The free length of the model shaft
- Its ratio m'/EI

The damping device used for safety reasons in the full scale shaft design (figure 9) was adopted from the tail rotor drive shaft of Eurocopter's EC120[12] helicopter.

2.3 Detailed Shaft Design

The dimensions and the mass and stiffness properties of the full scale TRISYD ICS resulted in a Cauchy number of approximately 460.

As for the length of the model shaft, it appeared reasonable to implement a shaft length of one segment (between two bearings) close to the one of the full scale ICS. This led to a characteristic length of slightly more than 2 m.

Thus, with the Cauchy number mentioned above, the ratio m'/EI had to have the following value:

$$\frac{m'}{EI} = 9.5\text{x}10^{-5}\ \text{s}^2/\text{m}^4. \tag{9}$$

As the inner diameter and the wall thickness and thus (with the known density of the CFRP material) the distributed mass per meter were already fixed, the needed modulus of elasticity E ("Young's modulus") was calculated:

$$E \approx 54\ \text{GPa}. \tag{10}$$

Differently from any metal, which shows only a very small variation of E (depending from the alloy), the effective modulus of elasticity of a CFRP material can be "tailored" by selecting the numbers of 0°, ±45°, and 90° layers in the used CFRP fabric.

For a CFRP shaft, the following relations hold (see also [6]):

- Layers with fibres parallel to the shaft axis (0° layers) mainly provide the shaft bending stiffness and strength.
- Layers with a ±45° angle with respect to the shaft axis (±45° layers) are needed to achieve a satisfactory torsional stiffness and strength.
- A high modulus of elasticity (with respect to shaft bending) can only be achieved at the expense of a low shear modulus, and vice versa.
- The use of 90° layers reduces both the bending and the torsional stiffness of the shaft. However, a certain fraction of 90° layers is necessary for a shaft in order to improve the overall strength of the shaft.

As the diagonal layers have a distinctly lower modulus of elasticity (Young's modulus) than the 0° layers, the effective value of Young's modulus with respect to shaft bending decreases along with the amount of diagonal layers in the CFRP material. This dependency is shown in figure 10, which is based on basic calculations performed at Eurocopter. This calculation assumed a CFRP shaft without 90° fibres.

[12] EC120 = Eurocopter single engine light helicopter with MTOW = 1800kg

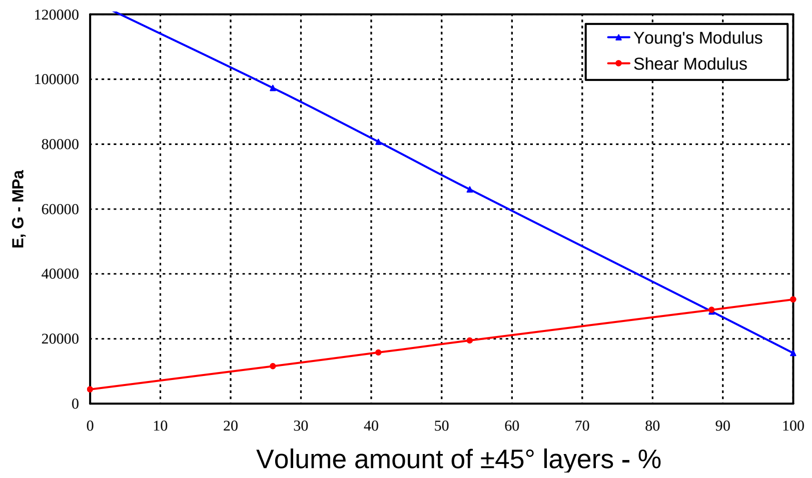

Figure 10: Influence of amount of 45° layers on effective Young's modulus of compound CFRP

By interpolating in this diagram, it can be seen that the model shaft needs a high fraction of diagonal layers of about 65%. This fraction is achieved by combining ±45° layers and 0° layers as shown in the figure 11.

The used laminate is balanced and symmetric. The composite tubes are fabricated using a fabric winding process. The sectional composition of the shaft is described in figure 11.

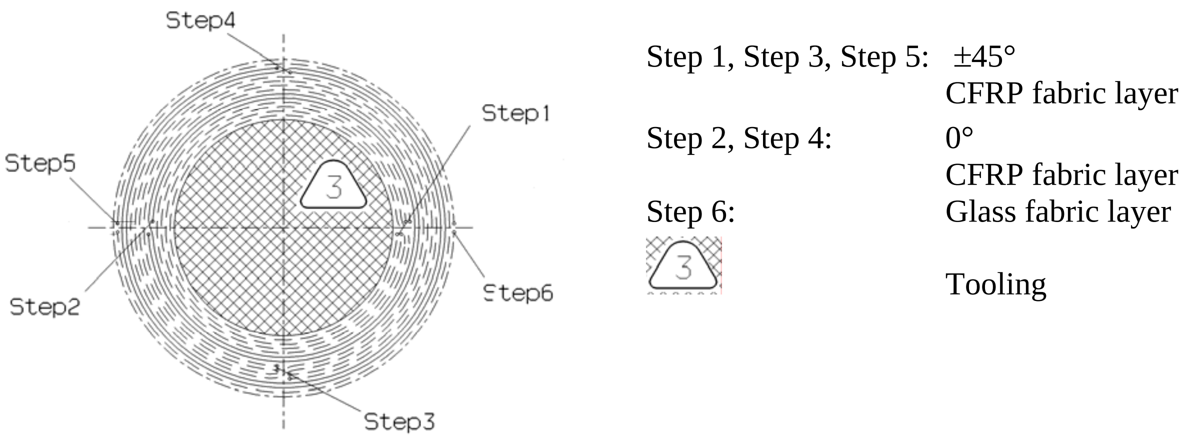

Figure 11: Sectional design and manufacturing steps of the CFRP-shaft

The resulting downscaled model of the ICS with its common helicopter tail rotor drive shaft components like flanges, flexible couplings and the damper is shown in figure 12.

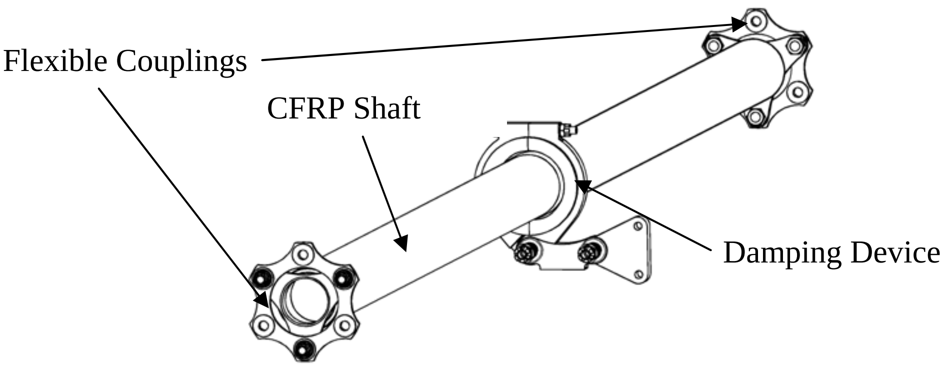

Figure 12: Downscaled model shaft with damping device

The calculated first natural frequency of the downscaled ICS is $\omega_1 = 36$ Hz.
The nominal frequency of the shaft (100%) is $\Omega_{100\%} = 83$ Hz.

3 DOWNSCALED SHAFT TESTING

3.1 Definition of the Test Bench

The aim of the interconnecting shaft (ICS) test campaign was to investigate the following:

- Study of the shaft behaviour when passing the first critical speed
- Confirmation of the theoretical calculations
- Determination of actual damping values
- Analysis of the influence of the bearing support damping

The influence of damping on the shaft behaviour is shown in figure 13. It depicts the stability limit for a Laval rotor (also called Jeffcott rotor) as a function of the ratio Ω/ω_1 of relative rotor speed (i.e. the shaft operating speed) to shaft speed (i.e. the shaft first critical speed), to the ratio D_a / D_i of outer damping D_a (damping in the fixed system) to inner damping D_i (damping in the rotating system).

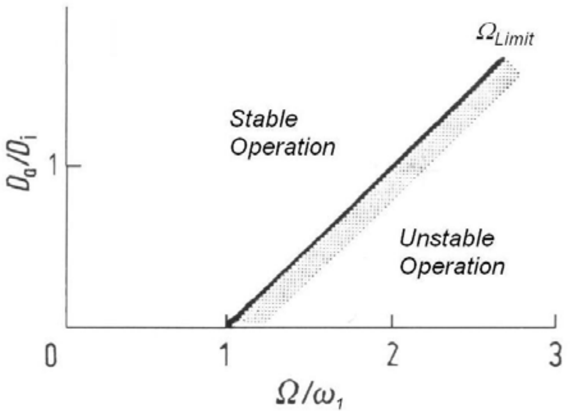

Figure 13: Stability limit of the test shaft with assumed stiff bearings

Assuming stiff bearings, the diagram is also valid for the ICS test bench. The frequency ratio for the downscaled ICS is:

$$\Omega_{100\%} / \omega_1 = 2.3 \qquad (11)$$

According to this ratio a ratio $D_a / D_i > 1$ is necessary (see figure 13). The analysis of the damping revealed that stiff bearings for the ICS test bench may lead to an unstable operation of the shaft. Therefore additional external damping was introduced by installing the bearings on elastomeric suspension blocks. With this solution, anisotropic bearing stiffness properties in vertical and lateral shaft directions were obtained.

The test bench design included the definition of the measuring device and sensors leading to the following characteristics:

- A hydraulic drive engine able to achieve the required accelerations, speeds and torques
- Two test bench specific shafts with flexible couplings for dynamically separating of the test shaft from the driving and torque absorption unit
- Bearing supports with elastomeric damping sheets and three-dimensional piezo force sensors.
- A damper device as designed in figure 12
- An intermediate prototype gearbox for torque absorption
- Speed, torque and displacement sensors on the middle of the shaft

Figure 14 shows a schematic drawing and a photo of the test bench, which was assembled on one of Eurocopter’s span areas.

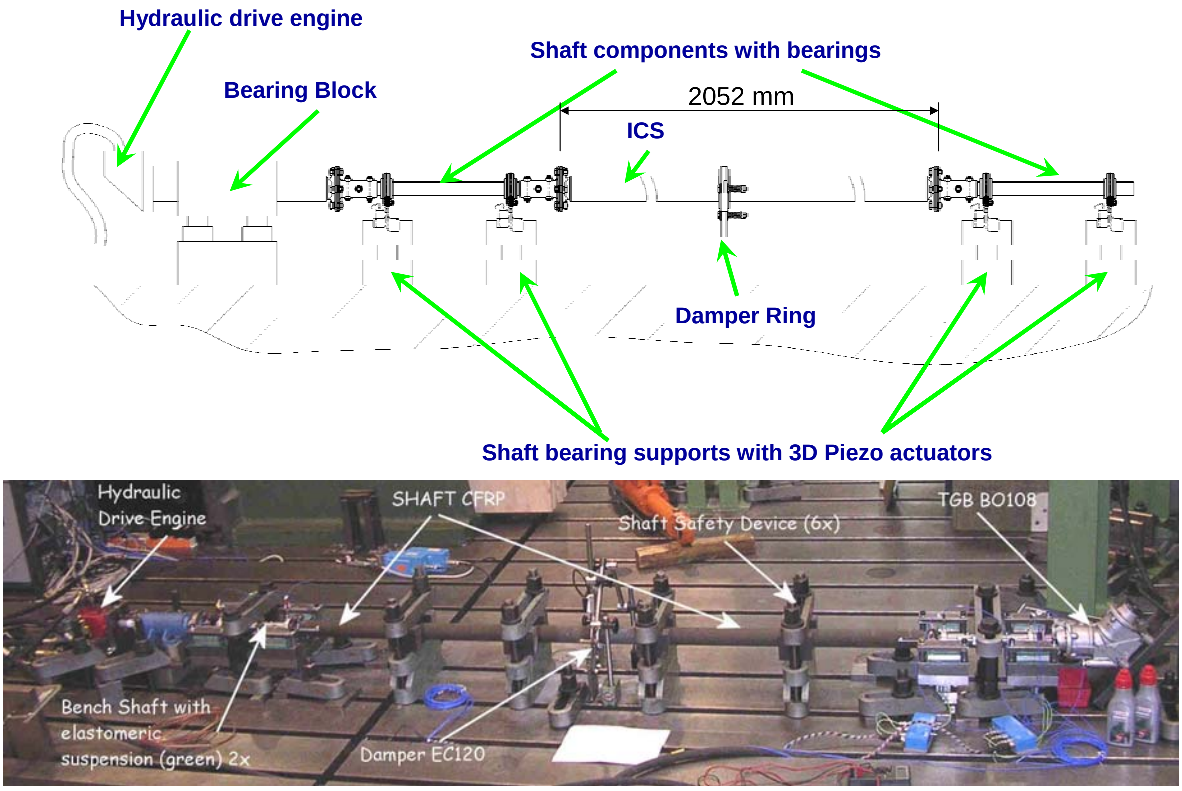

Figure 14: Test bench layout for interconnecting shaft testing

The shaft was made of two CFRP segments. It was statically and dynamically well balanced. All attaching components like adapters, flanges, couplings, damper and a torque absorbing gearbox are helicopter tail rotor drive components.

3.2 Performed Tests

During the test campaign, bang tests were performed to determine the shaft frequency and the damping behavior as follows:
- Bang tests with isolated shaft tubes supported by ropes (free-free)
- Bang tests with the complete shaft installed on the test bench (figure 14) during standstill
- Bang tests at different shaft speeds

Run-ups were also performed to determine the basic shaft behavior and to confirm the 1st bending frequency. Unbalance and misalignments were introduced to determine the sensitivity of the shaft in real environment conditions.

All tests with rotating shaft were performed with a tail gear box for torque reaction. A list of the main performed tests is shown in table 5.

Table 5: List of performed tests of the ICS

No.	Tests with Elastomeric supported bearings
1	Bang-Tests at Standstill in Y- and Z-Direction
2	Run-up till max. 100 Hz with acceleration variation
3	Run-up till max. 100 Hz with unbalance
4	Run-up till max. 100 Hz with misalignment
5	Bang-Tests at different speeds
	Tests with Stiff supported bearings
6	Run-up till max. 100 Hz

3.3 Test Results

The bang tests were performed by exciting the shaft with a hammer, and by subsequent analysis of the time history.

For the first bang tests of the “free-free” shaft segments the analysis yielded a damping ratio of 0.2%. This value was determined based on the acceleration time history using the formula

$$\zeta = \frac{\ln 2}{\omega_0 T_H} \tag{12}$$

with the damping ratio ζ, the natural frequency ω_0 and the time to half amplitude T_H . This result was in good agreement with the preliminary estimations. An example for the measured time history of the shaft end acceleration of such a bang test is shown in figure 15.

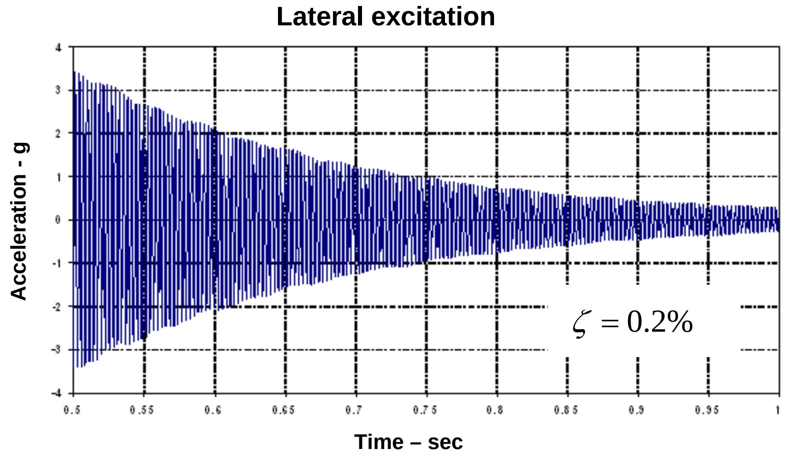

Figure 15: Bang tests with one isolated shaft tube (“free-free”)

The damping of the complete shaft on the test rig differs in lateral and vertical direction due to the anisotropic characteristics of the elastomeric damping elements under the bearings. Figure 16 shows the acceleration on one bearing during bang tests on the test bench at standstill with lateral and vertical excitation.

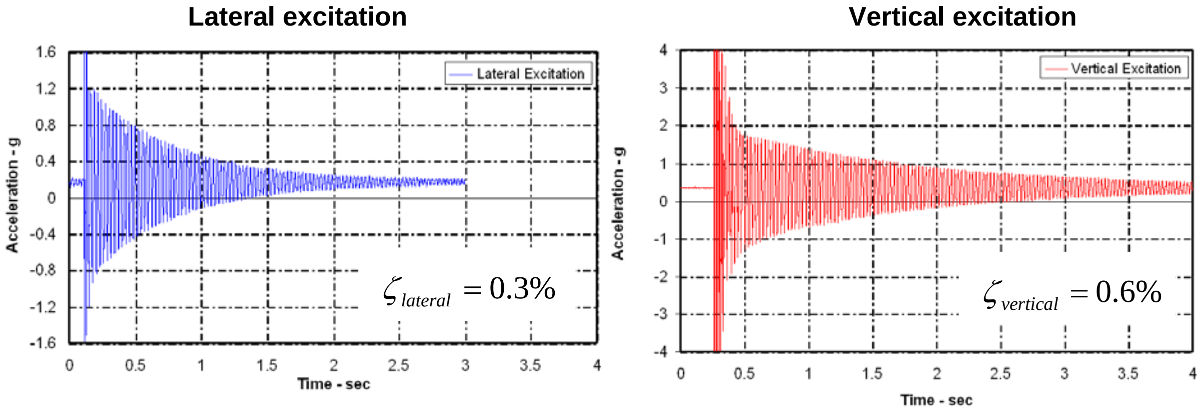

Figure 16: TRISYD test rig: bang-tests with shaft at standstill

In lateral direction a higher damping and a slightly reduced natural frequency was obtained compared to the vertical direction. With the vertical excitation a double damping amount was obtained compared to a lateral excitation.

Additional bang tests were performed with rotating shaft using lateral and vertical excitation. Figure 17 shows the time history of the mid-shaft displacement during a test with lateral excitation at a shaft speed of 6000 rpm (100 Hz). It can be observed, that the lateral displacement faded away earlier than the vertical displacement of the shaft. An energy transfer between the two oscillation directions can be observed which is favoured by the damping anisotropy.

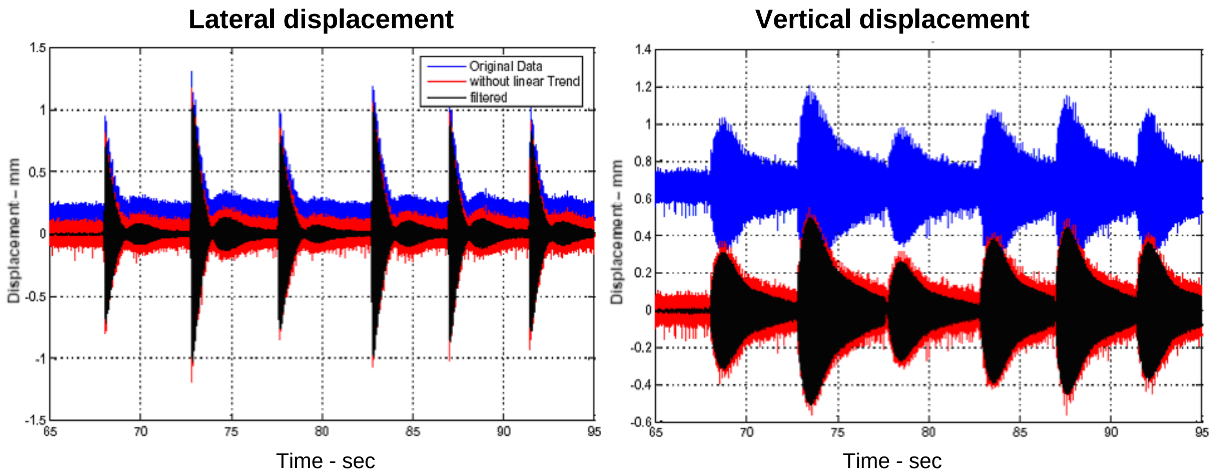

Figure 17: Bang tests with lateral excitation at 100 Hz

The displacement time history of a test with vertical excitation at 100 Hz is shown in figure 18.

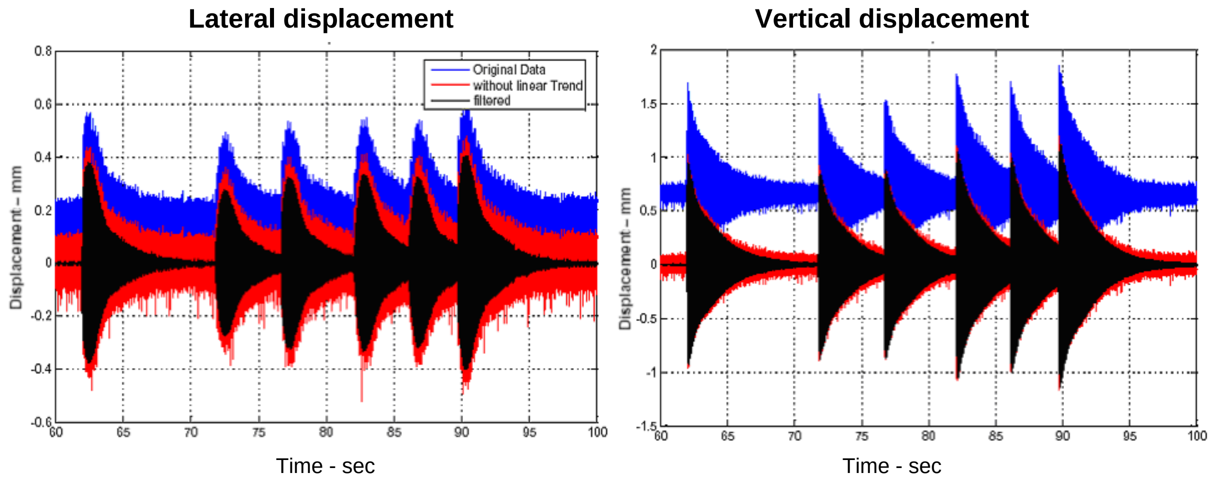

Figure 18: Bang tests with vertical excitation at 100 Hz

Due to the anisotropic bearing suspension damping, the shaft behaviour was confirmed on rotating shaft tests. The vertical oscillations are distinctly smaller than the lateral ones. The relation to the damping anisotropy is hereby shown.

One main aim of the tests was to perform run-ups up to nominal shaft speed and above. The calculated 1st critical speed of the downscaled shaft was 36 Hz (2160 rpm). The shaft was balanced at 1800 rpm. The crossing of the 1st critical speed was performed successfully for different accelerations. The analytical prediction of the critical speed was confirmed by the test with a 1st critical speed of about 35 Hz (2100 rpm). The result of the run-up is shown in figure 19.

The supercritical amplitudes of the shaft appear to be smaller than the subcritical ones due to the self-centering behaviour of the shaft and to the well-damped bearing suspension.

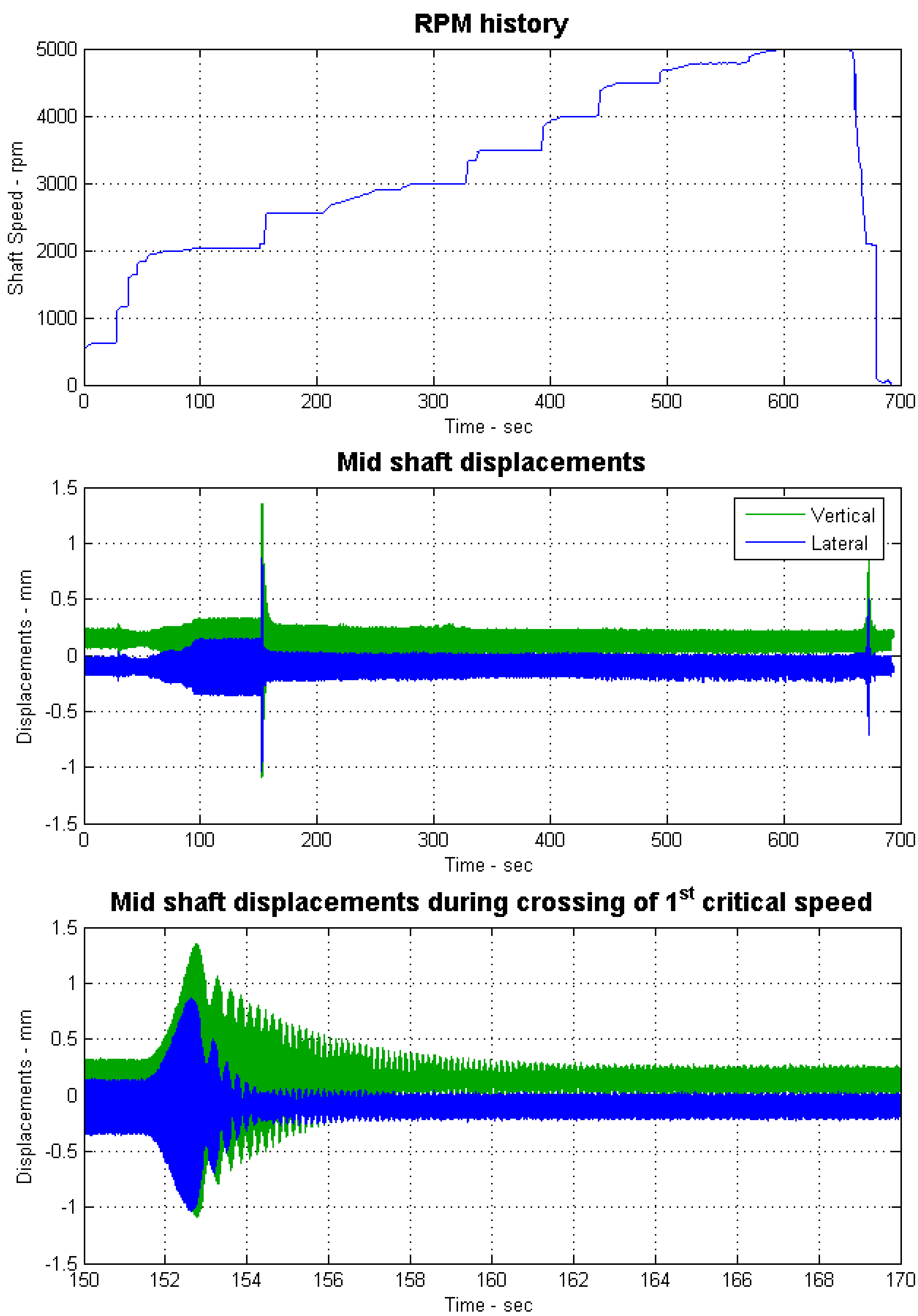

Figure 19: Supercritical run-up above the nominal shaft speed with balanced, aligned shaft and elastomeric supported bearing suspension

The implementation of shaft unbalance up to 4 g on the shaft outer diameter as well as of axial misalignments up to 20 mm and angular misalignment up to 1° still showed a smooth behavior of the shaft. The shaft displacements during the misalignment tests were similar to the run-up shown in figure 19. Only during the tests with a higher unbalance a contact between damping device and shaft could be observed when crossing the critical shaft speed. However, this contact quickly stopped as soon as the shaft had passed the 1st critical speed.

Finally, the shaft behavior with stiff, non-damped bearings was investigated. A run-up with this configuration is presented in figure 20. In this case, the supercritical shaft displacement amplitudes are distinctly higher than the subcritical ones. After passing of the first natural frequency the shaft displacements remained on a high level. Obviously, there was contact between the mid shaft and the damping device which limited the shaft displacements.

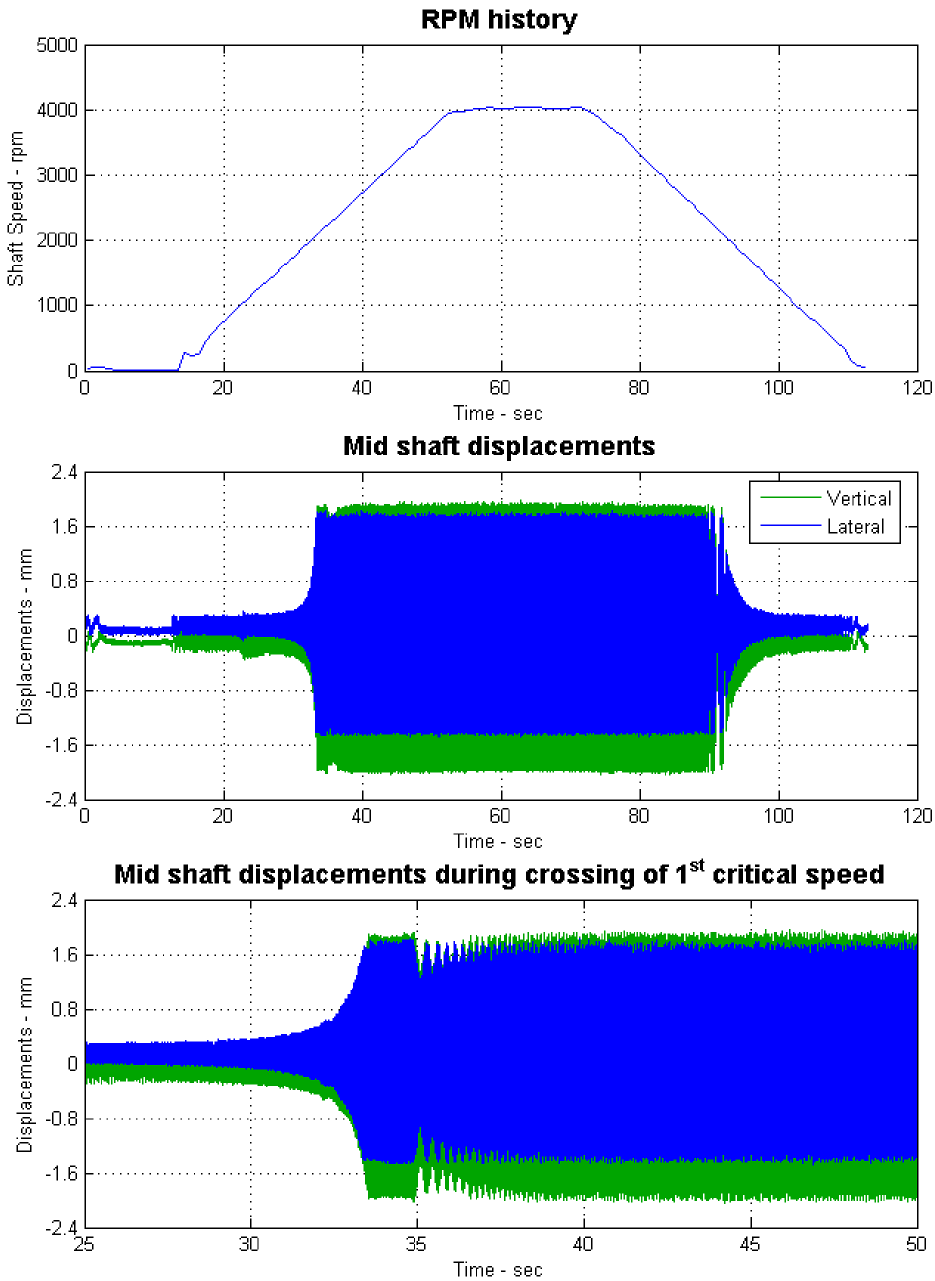

Figure 20: Supercritical run-up above the nominal shaft speed with balanced, aligned shaft and stiff bearing suspension

4 RECOMMENDATIONS FOR THE FULL SCALE SHAFT

Within the TRISYD project, it was decided to design a modern interconnecting shaft and to perform tests with a downscaled model of the shaft for finding a way of efficient preliminary tests for such a type of component. The design of the shaft led to a supercritical CFRP design. The manufacturing and testing of the shaft as a full scale model would have been very effort-intensive. Therefore, the downscaled model was manufactured and tested.

The aim of the tests was to examine the behaviour of the shaft and to derive recommendations for the full scale model of the shaft.

The following recommendations can be pointed-out for the full scale shaft:

- The defined design of the shaft shall be maintained due to the fact that the downscaling and the predicted, calculated shaft behaviour were confirmed by the tests.
- The shaft shall be designed as a supercritical shaft made of six equally spaced CFRP shaft segments with a length of 2200 mm per segment.
- The left and right wing shafts shall be dynamically separated by a short and stiff mid-wing segment.
- The installation of the shaft in the aircraft shall be made by supporting the bearings by means of elastomeric layers. The vibrations shall be hereby minimized outside of the rotating system. This leads to a reduced wear of components such as bearings or shafts.
- The fatigue behaviour of the elastomeric damping elements must be confirmed within long term tests and/or flight tests.

5 SUMMARY AND FUTURE VIEW

ERICA is a concept of an advanced tilt rotor aircraft having independently tilting nacelles as well as independently tilting outboard wing parts. The nacelles are connected by a rigid torque tube. The interconnecting shaft is connecting the two rotor gearboxes and is rotating inside this torque tube. Its purpose is to synchronize the rotors and to transmit the engine power from one engine to the opposite rotor in case of an engine failure. Within this paper, the development of the interconnecting shaft was shown.

The interconnecting shaft was designed as a supercritical shaft passing the 1st critical frequency. It was made from carbon fiber reinforced epoxy (CFRP) material and consists of six long and one short mid-wing segment. All segments are supported by roller bearings. The six long segments are equally spaced from bearing to bearing. The seventh segment is a short segment in the mid-wing section above the fuselage. Its purpose is to dynamically separate the left and right wing shafts.

For test purpose, a downscaled model of one shaft segment was manufactured and investigated. For safety reasons a damping device with a defined gap was introduced in the middle of the shaft. Special attention was paid to a new bearing support concept using elastomeric damper sheets.

The behavior of the shaft was investigated, especially regarding the following aspects:

- The passing of the critical frequency
- Confirmation of the predicted calculations (bang tests, critical frequency comparison)
- Study of the bearing support damping behavior

It can be concluded, that the behaviour of the shaft was successfully predicted by the calculations. Therefore, the results of the tests can be transferred to the full scale model of the shaft. The damping on all test bench bearings by means of elastomeric layers led to a very smooth behaviour of the shaft during and after passing the critical frequency. The passing of the critical frequency led to very low shaft displacements. The damping device in the middle of the shaft was not touched during run-up and run-down of the shaft. The shaft behaviour was very smooth. The following can be concluded: the use of elastomeric damping on the bearing support leads to low vibrations on the shaft during the whole necessary speed range.

In future, such a shaft system shall be used on the ERICA tilt rotor aircraft. The results can also be implemented on other rotorcraft long drive shaft applications.

REFERENCES

[1] Alli P: *Erica: “The European Tiltrotor. Design and Critical Technology Projects“* Agusta, Cascina Costa Di Samarate, Italy, AIAA-2003-2515
AIAA International Air and Space Symposium and Exposition: The Next 100 Years, Dayton, Ohio, July 14-17, 2003

[2] AC 29.931 (Amendment 29-12): *Shafting Critical Speeds*. Advisory Circular of the JAR, Part 29.931, Joint Aviation Authorities, Feb. 2002

[3] Dietz S.*, Wallrapp O.†, Wiedemann S.†: *Nodal vs. Modal Representation in Flexible Multibody System Dynamics,* MULTIBODY DYNAMICS 2003 Jorge A. C. Ambrósio (Ed.) IDMEC/IST, Lisbon, Portugal, July 1-4 2003

[4] Duello, C. “*BA609 Tiltrotor Drive System*”,
58th AHS Forum, Montreal, Canada, June 11-13, 2002

[5] Flemming, M., Ziegmann, G., Roth, S.: *Faserverbundbauweisen – Halbzeuge und Bauweisen.* Springer Verlag, 1996.

[6] Gasch, R., Nordmann N., Pfützner, H.: *Rotordynamik 2. Auflage,* Springer, Berlin, 2002

[7] JAR, Part 25: *Joint Airworthiness Requirements, Transport Category Aircraft.* Joint Aviation Authorities, Nov. 1993

[8] JAR, Part 29: *Joint Airworthiness Requirements, Transport Category Rotorcraft.* Joint Aviation Authorities, Nov. 1993

[9] JAR, Part 29.931: *Shafting Critical Speed. Joint Airworthiness Requirements, Large Rotorcraft.* Joint Aviation Authorities, Nov. 1993

[10] Kilmain, C. et al.“*V-22 Drive System Description and Design Technologies*”
51st AHS Forum, Ft. Worth, Texas, May 9-11, 1995

[11] Pestel E., Leckie F.: “*Matrix Methods in Elastomechanics*”
Mc Graw-Hill Inc., 1963